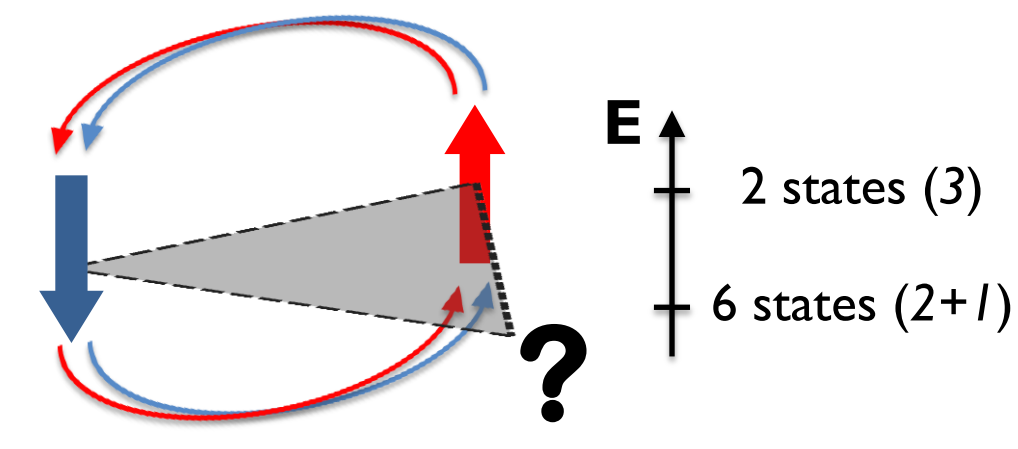
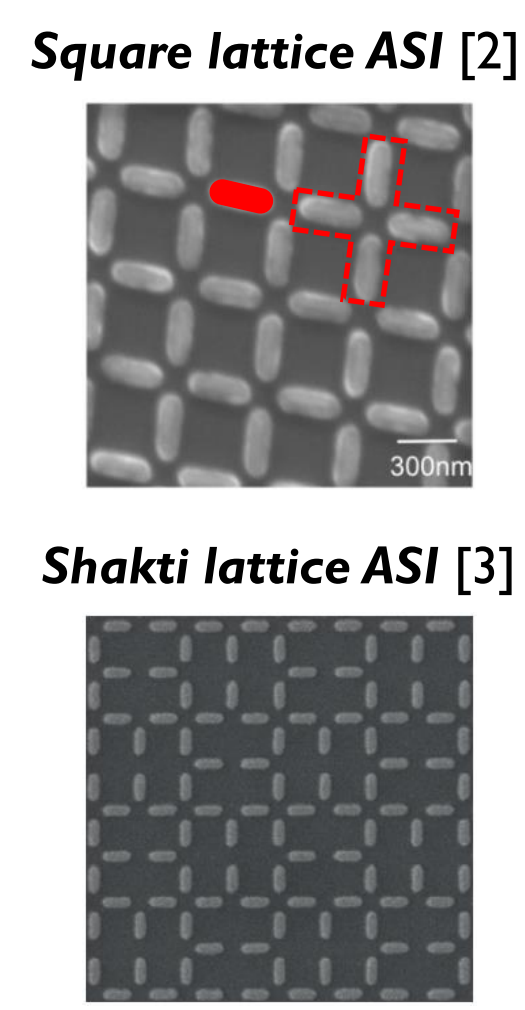


Introduction: Artificial Spin Ice

Introduced in 2006, Artificial Spin Ice (ASI) systems are metamaterials consisting of arrays of dipolar-coupled nanomagnets arranged in **frustrated geometries** [1].

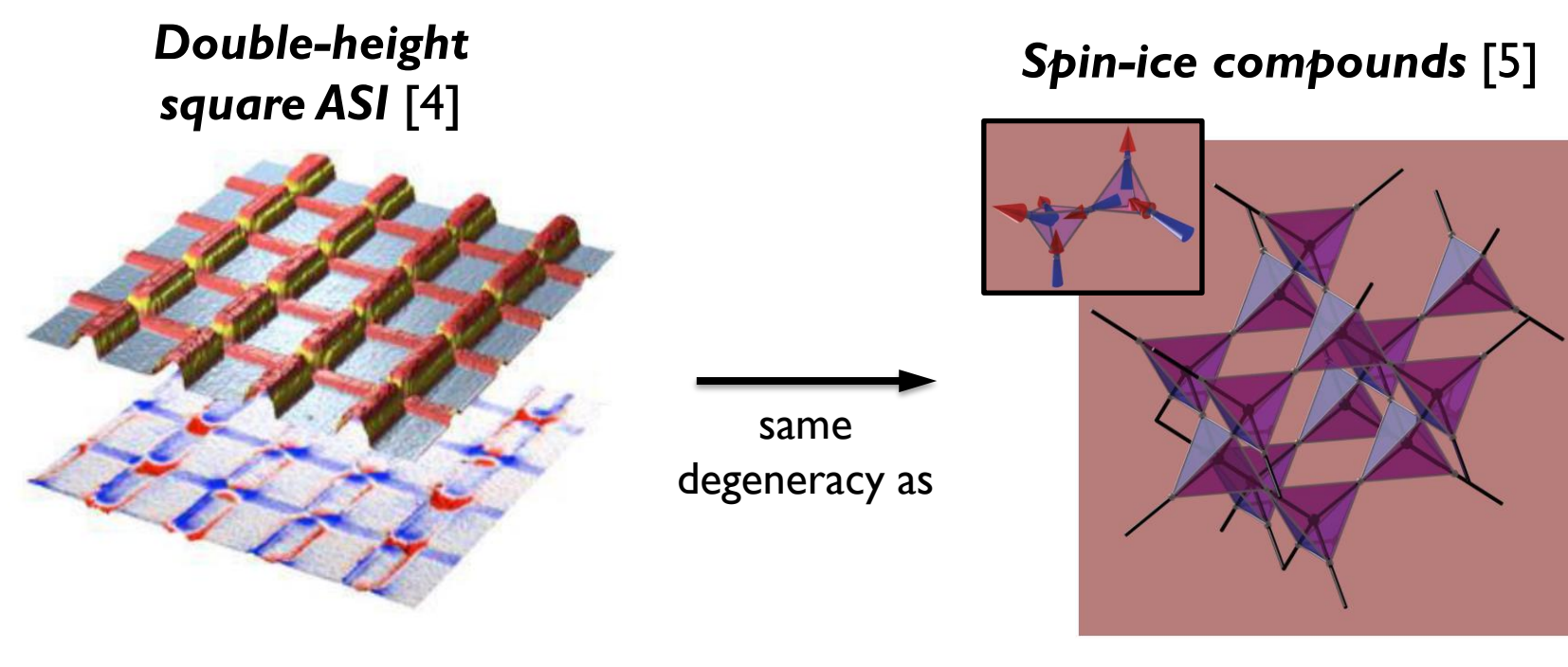


Frustration: the inability of a physical system to satisfy all the interactions simultaneously, leading to a large degeneracy of low-energy states.



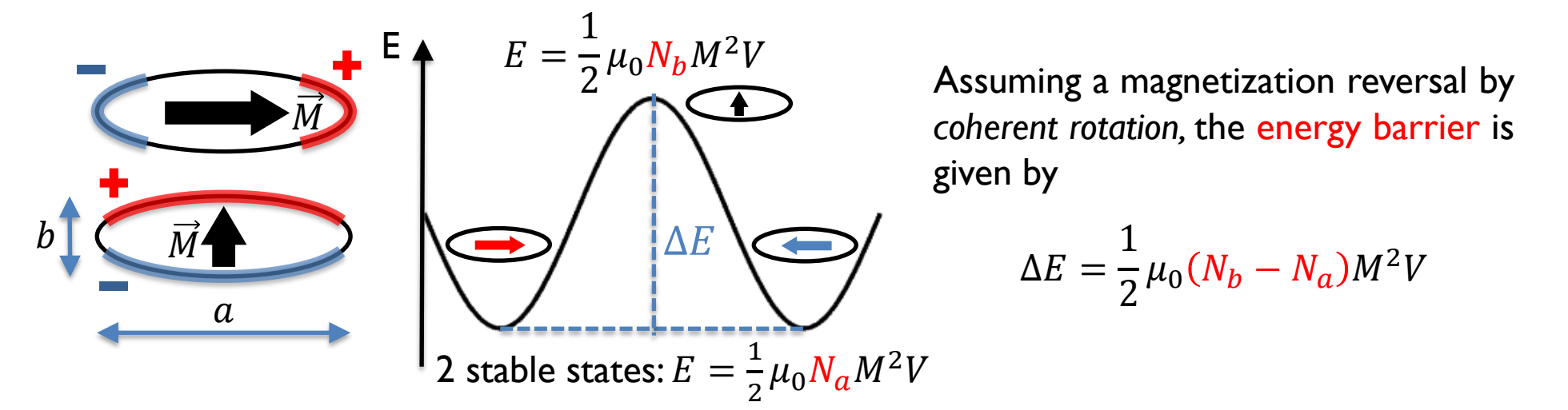
Interesting features

- 2D model systems in which the lowest-energy state can be obtained at **room temperature** and imaged through lab-scale imaging techniques (e.g., MFM, MOKE, LTEM);
- Advanced fabrication techniques (EBL) allow for the systematic variation of the key parameters governing the system (size, distance, arrangement, height offset, ...).

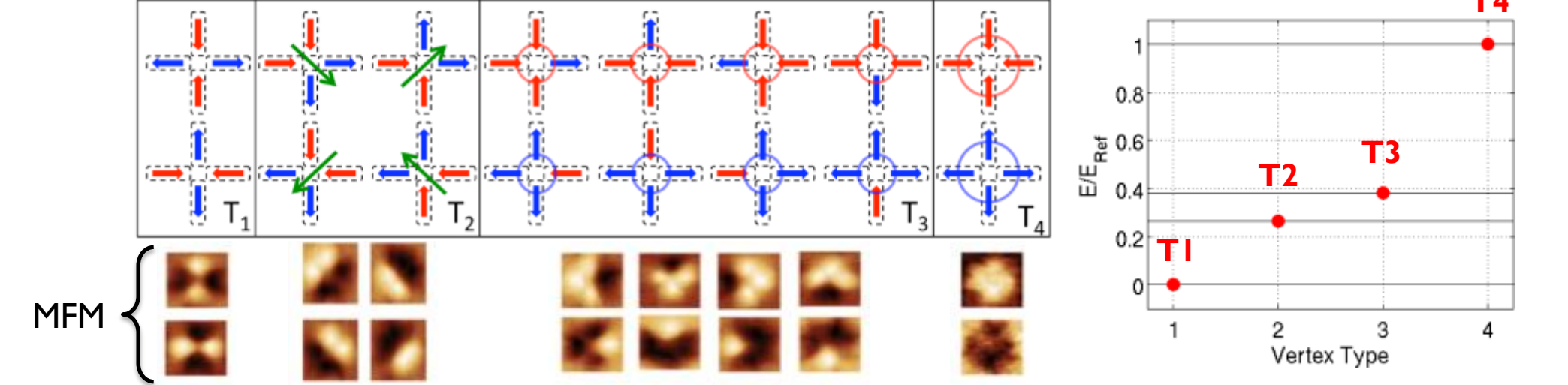


Key structures

- Base element: **Ising-like macrospin nanostructure**



- Base unit: **Vertex** (4 interacting nanostructures)



μm-scale: thermal protocol and kMC

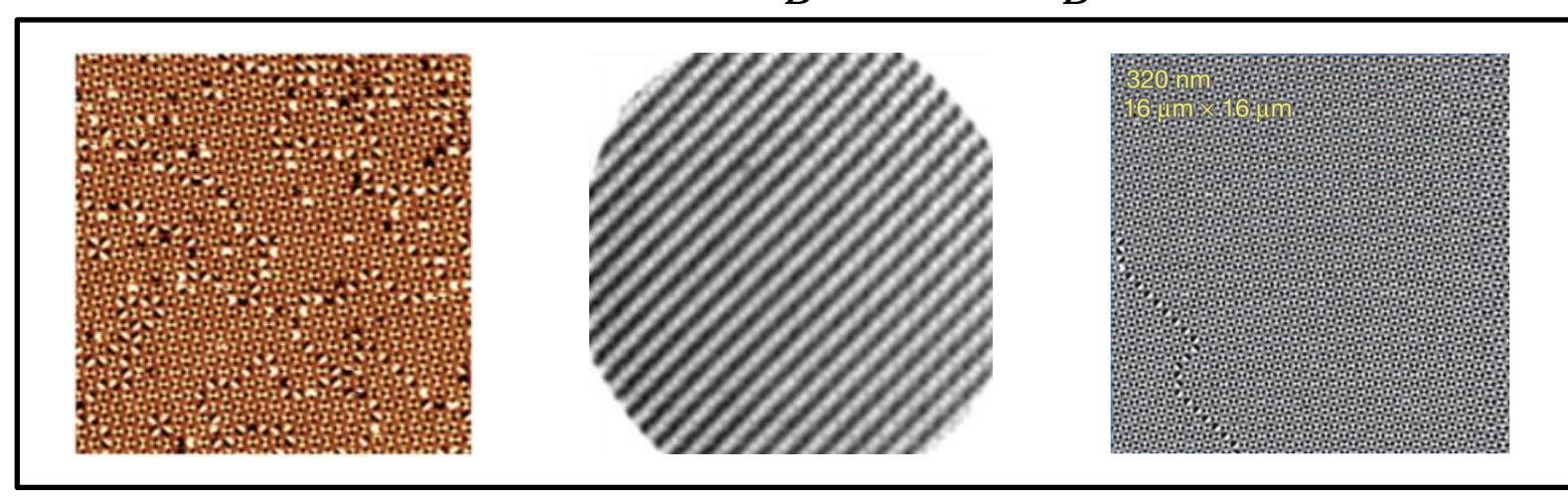
The **key process** in ASI systems consist in the formation of **low-energy states** (rarely observed): (1) the system is **melted** and (2) the frozen state (**equilibrium**) is recorded.

Demagnetizing protocol [2]



Thermal protocol [2,6,7]:

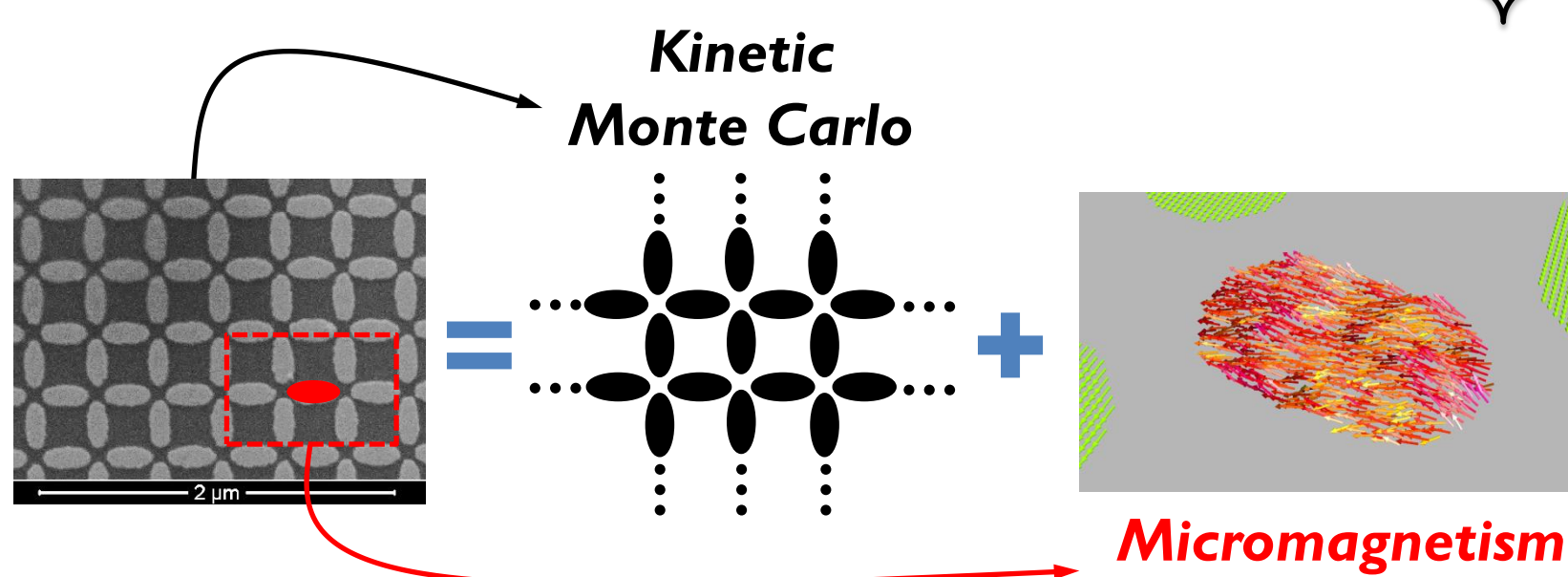
from $T > T_B$ to $T < T_B$



Bigger ground-state domains with respect to the demagnetizing protocol

The equilibrium configurations are usually simulated by Monte Carlo techniques [8], considering that

- Key structures:** Ising-like nanostructures (≤ 500 nm).
- Key process:** formation of low-energy states in extended systems ($\approx 20 - 50 \mu\text{m}$, so up to 10^4 nanostructures).

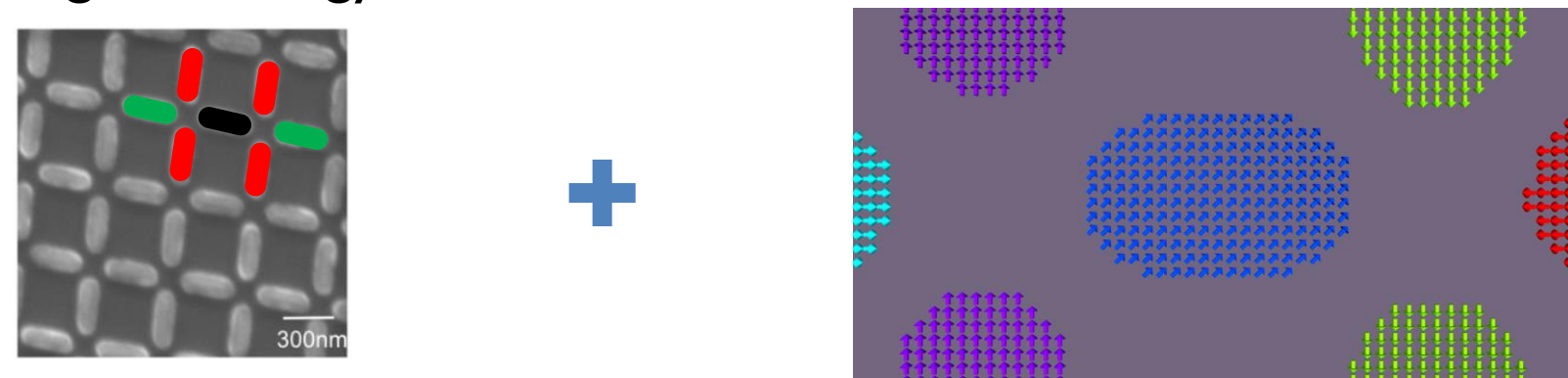


Our idea was to move a step further (beyond the macrospin approximation) and consider a **multiscale approach** (μm - and nm -scale):

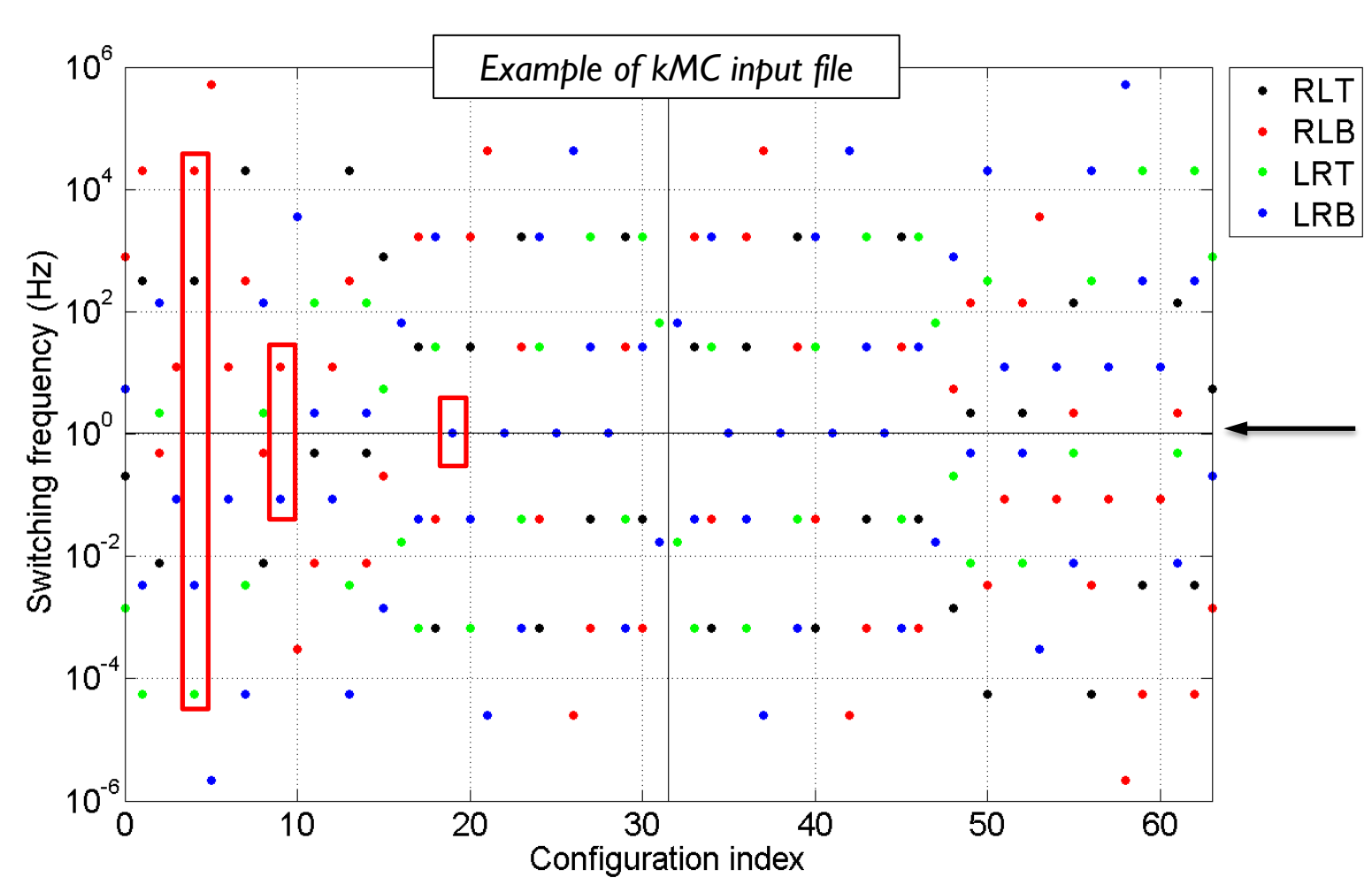
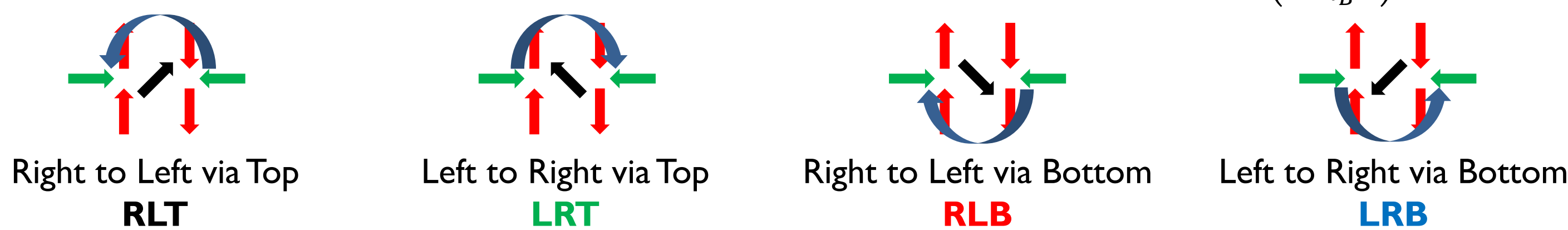
- Kinetic Monte Carlo (kMC)** combined with a more detailed analysis of the switching process;
- Micromagnetic analysis** of the thermally-induced magnetization reversal ($T \neq 0$ K).

Kinetic Monte Carlo [9] + precomputed switching frequencies

- The considered event is the magnetization reversal of a single nanostructure (**single flip**);
- The base unit is composed by 7 nanostructures (**center, first n.n.** and **second n.n.**);
- The 7 nanostructures are uniformly magnetized and the magnetization reversal in the central one occurs by **coherent rotation**, but the **actual shape** of the nanostructure is taken into account for calculating the energy barriers.



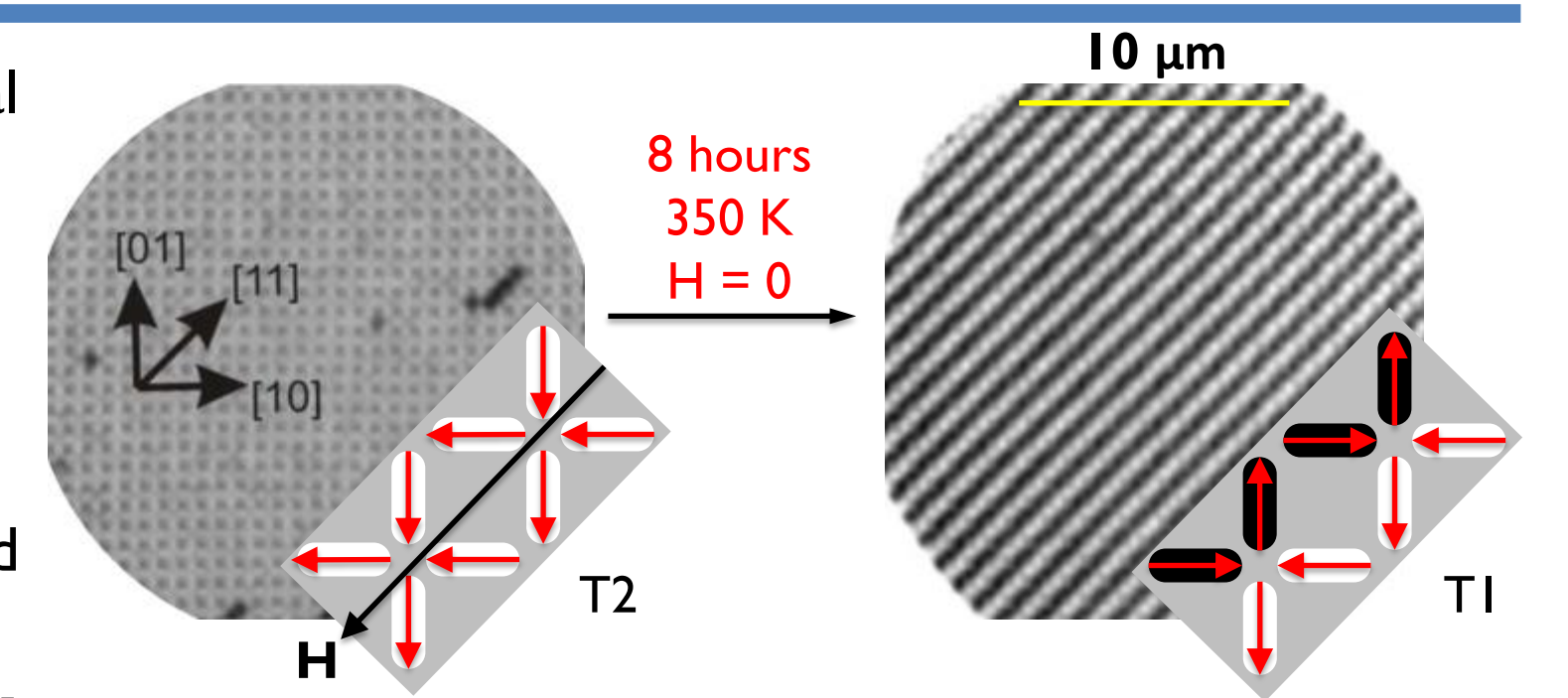
The input for the kMC consists in 64×4 switching frequencies $v_{sw}^i = v_0 \exp\left(-\frac{\Delta E_{CR}^i}{k_B T}\right)$:



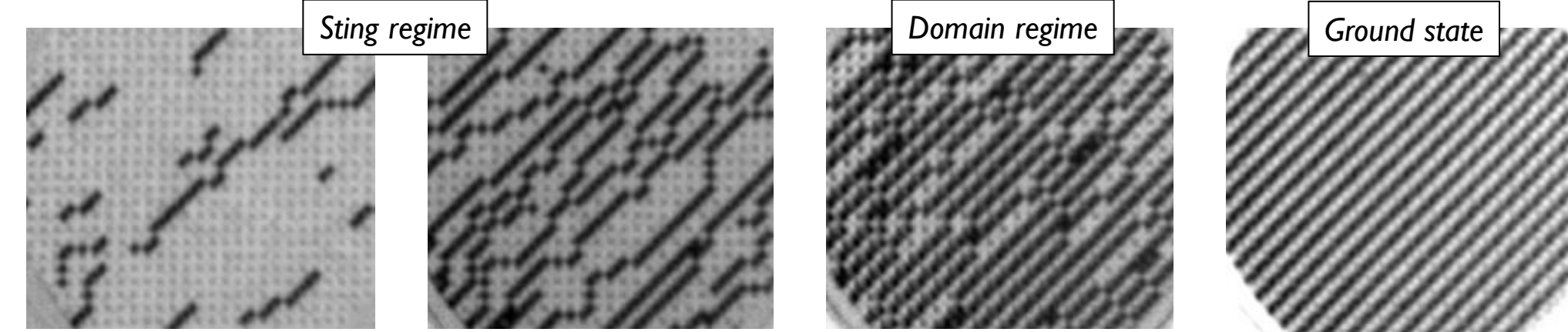
Switching frequency corresponding to ΔE_0 (energy barrier for the coherent reversal of an isolated nanostructure)

This approach allowed us to analyze experimental data available in literature [7]:

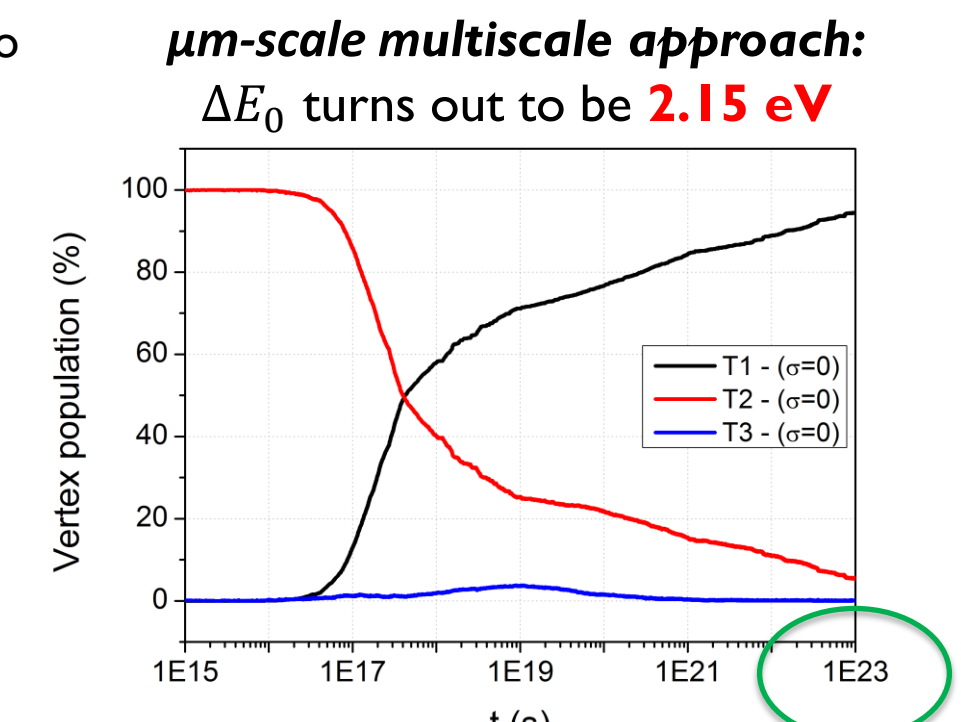
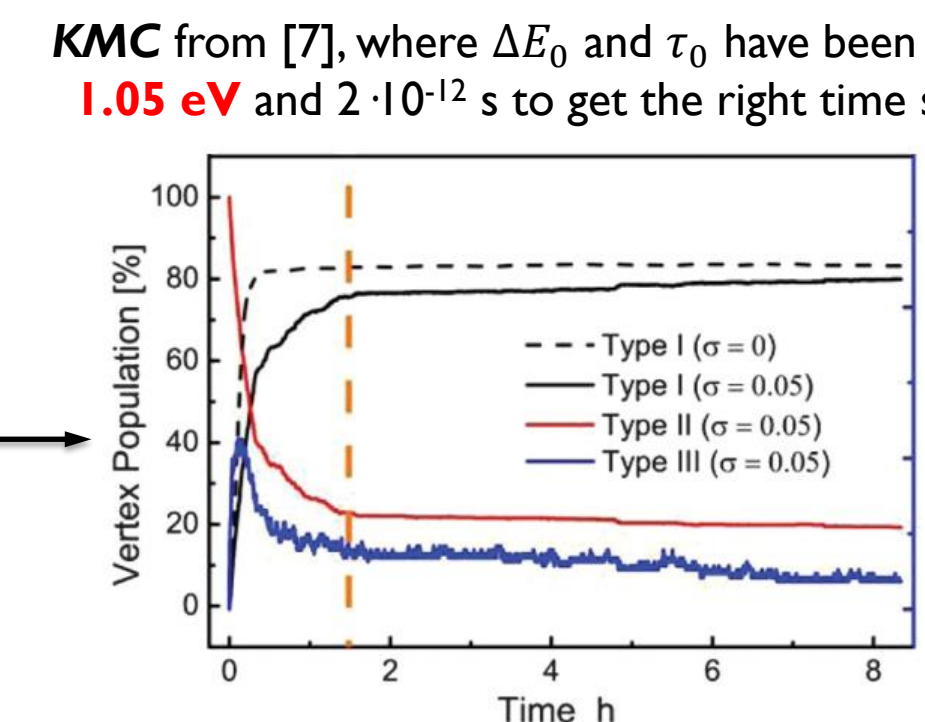
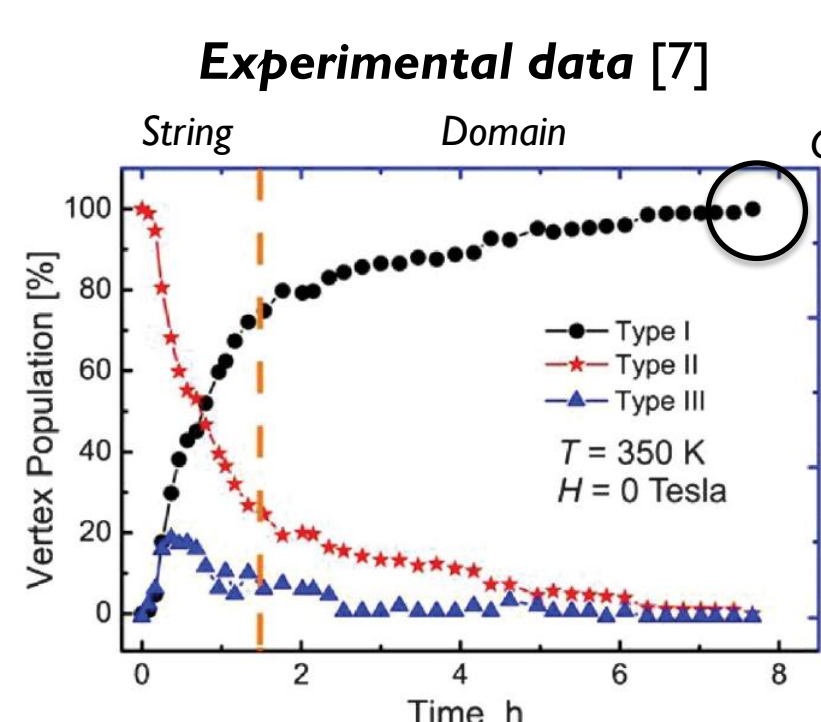
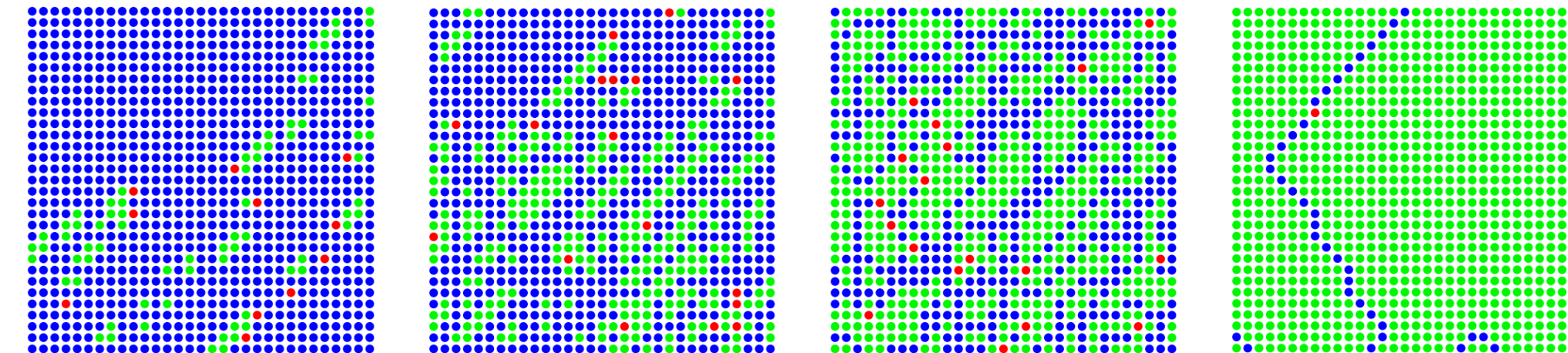
- $\text{Ni}_{83}\text{Fe}_{17}$
- $470 \text{ nm} \times 170 \text{ nm} \times 3 \text{ nm}$
- 130 nm edge-to-edge distance
- $M = 350 \text{ kA/m}$
- Sample saturated in a magnetic field applied along $[11]$ and measured by XMCD



Experimental data [7]



μm-scale multiscale approach

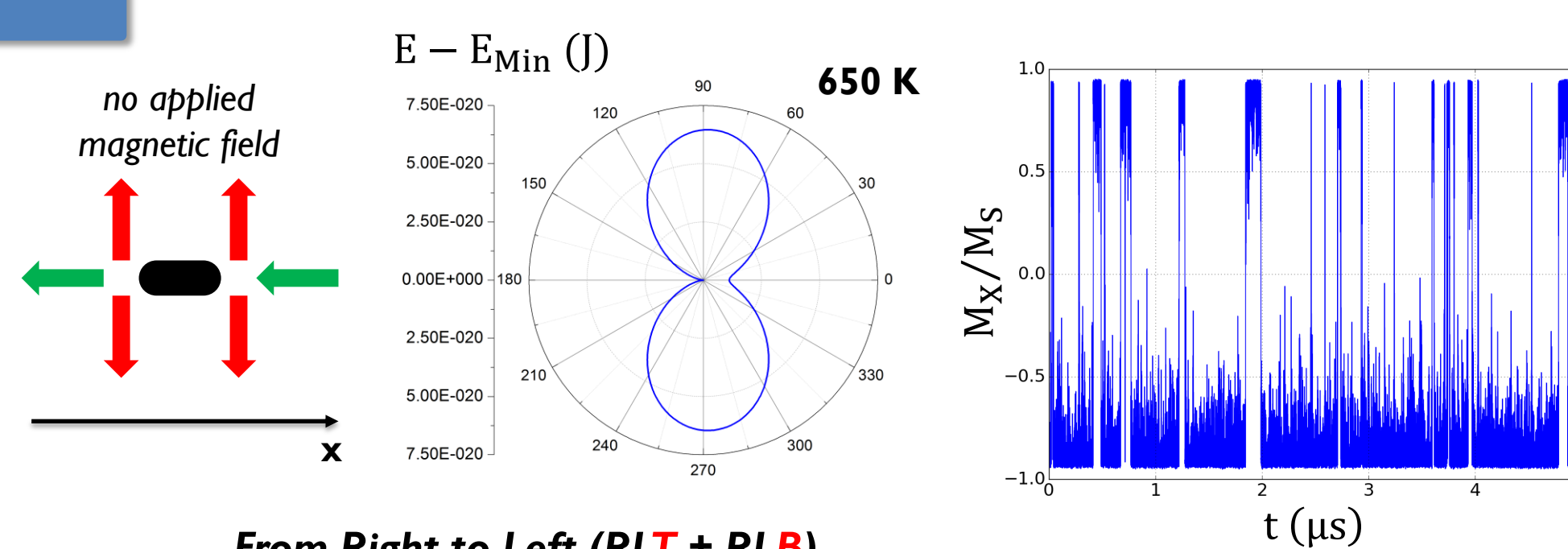
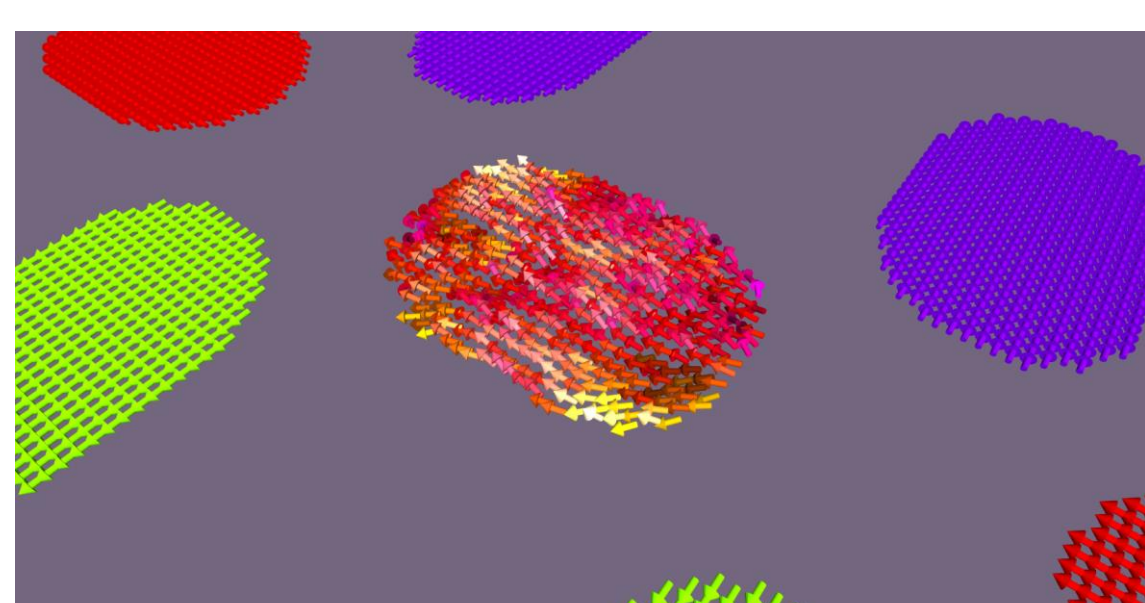


nm-scale: micromagnetism

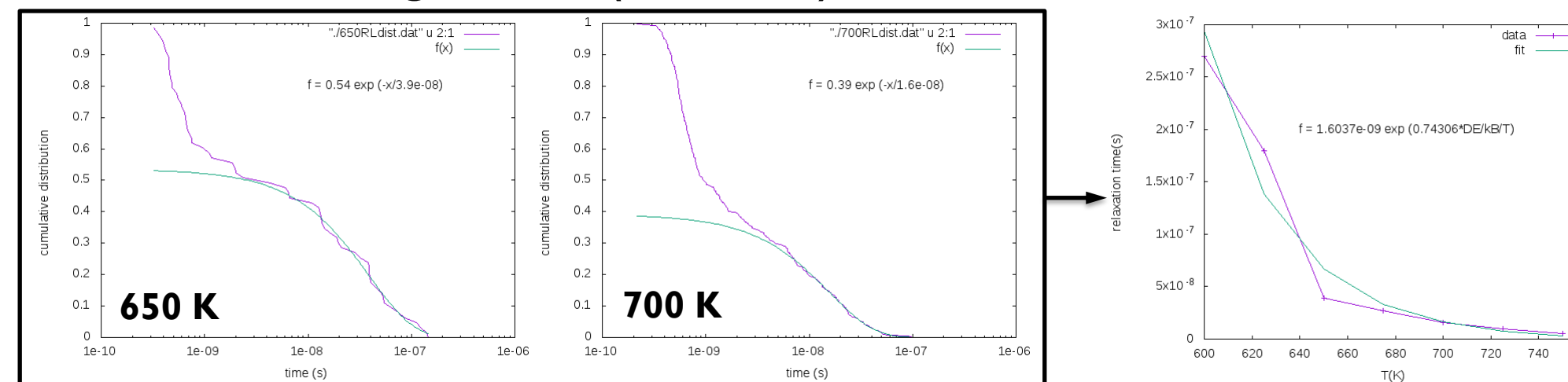
The difference in the kMC time scale (given by the energy barrier's difference) led us to consider a better approach for the magnetization reversal modelling at $T \neq 0$ K.

Micromagnetism

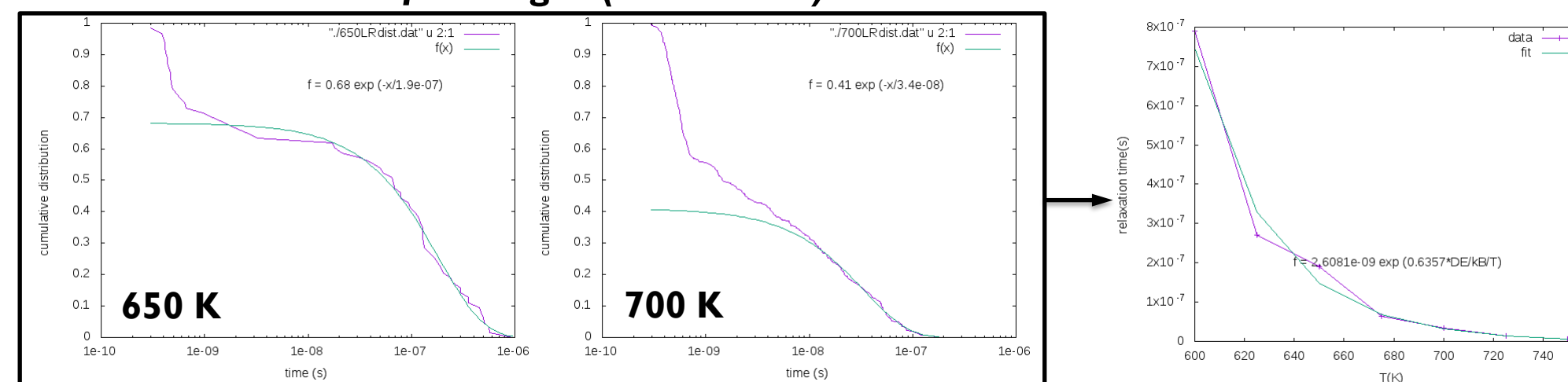
- Stadium-like Permalloy nanostructures ($150 \text{ nm} \times 100 \text{ nm} \times 3 \text{ nm}$) with $5 \times 5 \times 3 \text{ nm}^3$ cell volume;
- Analysis of the central nanostructure time evolution with **fixed magnetization** in the 6 n.n.;
- 5th order Runge-Kutta scheme with 4th order error correction [10] and **adaptive timestep**;
- At each temperature, $10 \mu\text{s}$ have been simulated and M_s has been accordingly **adjusted**.



From Right to Left (RLT + RLB)



From Left to Right (LRT + LRB)



$$\tau^i = \tau_0^i \exp\left(\frac{c^i \Delta E_{CR}^i}{k_B T}\right), \text{ where } \Delta E_{CR}^i \text{ is the coherent reversal energy barrier for configuration } i$$

Configuration (i)	Transition	τ_0^i (ns)	c^i
(0)	LRB	3.5 ± 0.6	0.61 ± 0.03
	LRT	2 ± 1	0.63 ± 0.12
	RLB	2.6 ± 0.7	0.62 ± 0.07
	RLT	-	-
(9)	LR	2.6 ± 0.8	0.63 ± 0.04
	RL	1.6 ± 0.7	0.74 ± 0.08
(16)	B	2.0 ± 0.3	0.71 ± 0.03
	T	2.2 ± 0.6	0.51 ± 0.04
(19)	-	3.0 ± 0.7	0.59 ± 0.03
		2.320 ± 0.003	0.6322 ± 0.0002

Conclusions

- We showed that, at high temperature (T close to T_B), the energy barrier can be about 63 % of the coherent reversal energy barrier and τ_0 lies in a range consistent with literature data. Anyway, a general analysis including room T is still missing (*future outlook*).
- The whole work points out the necessity of considering both the actual nanostructure's shape and the effect of temperature in order to calculate the proper energy barrier.

References

[1] R. F. Wang et al., *Nature* **439**, 303 (2006).
[2] J. M. Porro et al., *New J. Phys.* **15**, 055012 (2013).
[3] I. Gilbert et al., *Nature Phys.* **10**, 670 (2014).
[4] Y. Perrin et al., *Nature* **540**, 410 (2016).
[5] C. Castelnovo et al., *Nature* **451**, 42 (2008).
[6] S. Zhang et al., *Nature* **500**, 533 (2013).
[7] A. Farhan et al., *Phys. Rev. Lett.* **111**, 057204 (2013).
[8] Z. Budrikis et al., *New J. Phys.* **14**, 035014 (2012).
[9] A. B. Bortz et al., *J. Comp. Phys.* **17**, 10 (1975).
[10] A. Vansteenkiste et al., *AIP Advances* **4**, 107133 (2014).

Acknowledgements

We acknowledge support from the Basque Government (Project No. PI2015-1-19) and from MINECO, the Spanish Ministry of Economy and Competitiveness (Project No. FIS2015-64519-R and Grant No. BES-2013-063690).